Lab on a Chip

Accepted Manuscript

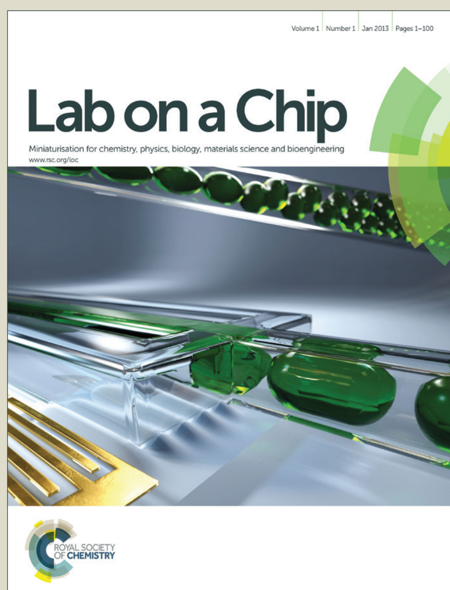

This is an *Accepted Manuscript*, which has been through the Royal Society of Chemistry peer review process and has been accepted for publication.

Accepted Manuscripts are published online shortly after acceptance, before technical editing, formatting and proof reading. Using this free service, authors can make their results available to the community, in citable form, before we publish the edited article. We will replace this *Accepted Manuscript* with the edited and formatted *Advance Article* as soon as it is available.

You can find more information about *Accepted Manuscripts* in the Information for Authors.

Please note that technical editing may introduce minor changes to the text and/or graphics, which may alter content. The journal's standard Terms & Conditions and the Ethical guidelines still apply. In no event shall the Royal Society of Chemistry be held responsible for any errors or omissions in this *Accepted Manuscript* or any consequences arising from the use of any information it contains.

ROYAL SOCIETY OF CHEMISTRY

www.rsc.org/loc

Fabrication of IR-transparent microfluidic devices by anisotropic etching of channels in CaF_2

*Brynson Lehmkuhl, Scott D. Noblitt, Amber T. Krummel, Charles S. Henry**

Department of Chemistry, Colorado State University, Fort Collins, Colorado 80523-1872, United States

*Corresponding author, chuck.henry@colostate.edu, 970-491-2852

KEYWORDS: IR transparent microfluidic device, calcium fluoride, microfluidics, hydrogen-deuterium exchange

Lab on a Chip Accepted Manuscript

Abstract

A simple fabrication method for generating infrared (IR) transparent microfluidic devices using etched CaF_2 is demonstrated. To etch microfluidic channels, a poly(dimethylsiloxane) (PDMS) microfluidic device was reversibly sealed on a CaF_2 plate and acid was pumped through the channel network to perform anisotropic etching of the underlying CaF_2 surface. To complete the CaF_2 microfluidic device, another CaF_2 plate was sealed over the etched channel using a 700-nm thick layer of PDMS adhesive. The impact of different acids and their concentrations on etching was studied, with HNO_3 giving the best results in terms of channel roughness and etch rates. Etch rate was determined at etching times ranging from 4-48 hours and showed a linear correlation with etching time. The IR transparency of the CaF_2 device was established using a Fourier Transform IR microscope and showed that the device could be used in the mid-IR region. Finally, utility of the device was demonstrated by following the reaction of N-methylacetamide and D_2O, which results in an amide peak shift to 1625 cm^{-1} from 1650 cm^{-1}, using an FTIR microscope.

Lab on a Chip Accepted Manuscript

Introduction

Fourier transform infrared (FTIR) spectroscopy is an important technique used widely to characterize chemical structures and dynamics. The ability of FTIR to measure changes in bond vibrational energy enables tracking of changes in bonding environment, including bond formation or breaking as well as qualitative chemical analysis. Microfluidic devices offer advantages for studying chemical reactions based on their low reagent consumption, short mixing times relative to traditional glassware, and ability to control solution composition.[1-3] Coupling IR spectroscopy with microfluidics can provide a powerful tool for following chemical reactions.[4-7] Using a FTIR microscope connected to a focal plane array (FPA) along with microfluidics can improve this technique, by generating spatially resolved mapping of individual spectra along a channel. [5, 8-12] However, FTIR is rarely used in conjunction with microfluidics because the majority of substrates used in microfluidics are not transparent in the mid-IR region. In the last decade there has been a growing interest in fabricating devices with low absorbance in the mid-IR region using IR-transparent substrate materials such as CaF_2, BaF_2, and silicon.[8, 12-14] Microfluidic devices made from silicon have traditionally used deep reactive ion etching and/or acid etching to create channels in methods common to the integrated circuit industry.[4, 7, 11] While effective, deep reactive ion etching requires access to tools that are both expensive and not widely available. Alternatively, channels can be patterned using one of several additive methods where layers of material are patterned over a smooth IR-transparent material. Common additive methods include photoresist, 3D printing, polydimethylsiloxane (PDMS) molding, and addition of laser cut polymer membranes.[9, 10, 12, 15] Approaches that utilize additive fabrication techniques where the CaF_2 or BaF_2 is unaltered and channels are defined by sandwiching a patterned layer

Lab on a Chip Accepted Manuscript

of material between two polished plates do not require the same level of sophistication for fabrication, but also use less common fabrication and bonding methods.

An alternative technique used to fabricate IR-transparent microfluidic devices is to etch channels into the CaF_2 itself. Pan *et al.* created channels in CaF_2 by patterning the substrate with photoresist and etching the exposed CaF_2 with $Fe(NH_4)(SO_4)_2$.[16] The CaF_2 plate was aligned and sealed to another CaF_2 plate that contained access ports with an adhesive photoresist layer. To minimize absorbance background, the photoresist was patterned in the positive relief of the etched channel. The completed microchip capillary electrophoresis device was used to separate amino acids, which were detected using fluorescence. Pan's method successfully generated microfluidic channels, but required multiple photolithography steps, micron-scale alignment when sealing the two CaF_2 plates together, and layers of clear acrylic paint to protect the bottom and side areas of the CaF_2 not covered by photoresist.

Here, we present a method for fabricating IR-transparent microfluidic devices using a PDMS microfluidic channel network to deliver the etchant, nitric acid, to the CaF_2 surface, allowing definition of micron-sized channels in CaF_2. Our approach enables etch depth to be controlled based on etching time while also producing uniform channels. Furthermore, the method is attractive because it does not require precise alignment unlike photoresist and silicon fabrication methods. Another advantage over silicon devices is the visual transparency of CaF_2, which permits easier alignment of the microscopic field of view and identification of entrapped gas bubbles in the microfluidic channels. The use of PDMS microchannels made by soft lithography enables fabrication of intricate fluidic channels since the PDMS etching mask is easily molded from photoresist designs on Si wafers. After studying the effect of different etchants, nitric acid was selected because it gave the fastest etch with the smoothest channels.

Lab on a Chip Accepted Manuscript

Etch rates were also established and found to be linear as a function of time. Finally, as an example application, etched CaF_2 microfluidic devices were used to follow the reaction between D_2O and N-methylacetamide (NMA) using a simple Y-channel configuration.

Experimental

Materials. Sylgard 184 and its crosslinking agent (PDMS) was acquired from Dow Corning Corp (Midland, MI, USA), 2 mm thick CaF_2 plates from Crystran (Poole, UK), and toluene from Fisher (Fairlawn, NJ, USA). Nitric acid was purchased from Mallinckrodt Chemicals, Phillipsburg, NJ, USA) and 1 mm diamond-tipped drill bits from Diamond Pacific Tool Corp. (Barstow, CA, USA). D_2O, oxalic acid, and NMA were purchased from Sigma-Aldrich (St. Louis, MO, USA). Sulfuric acid, hydrochloric acid, and dimethyl sulfoxide (DMSO) were purchased from EMD Chemicals, Inc. (Gibbstown, NJ, USA). All solutions were prepared using 18.2 MΩ*cm (Millipore, Billerica, MA, USA) deionized water.

Etching CaF_2. A schematic of the CaF_2 device construction is given in Figure 1. The channel was etched using a PDMS (10:1 ratio of Sylgard to its cross-linking agent) template patterned by soft lithography with a 500-µm wide Y-channel and aligned onto a 25-mm diameter CaF_2 plate. The PDMS microfluidic devices were made using well-established soft lithography methods common to many microfluidic laboratories.[17, 18] A custom, 3D-printed clamping device was used to keep the PDMS in conformal contact with the CaF_2 during etching (Figure 1a-d). In the optimized system, 1.5 M nitric acid was pumped through the inlets of PDMS mold at 0.25 µL/min via an automated syringe system (LabSmith, Livermore, CA, USA). In this approach,

Lab on a Chip Accepted Manuscript

channels fabricated in PDMS were reversibly sealed over an unpatterned CaF_2 plate. After the etching was complete, the PDMS was removed, the surface thoroughly washed with ultrapure water, and the resulting channels analyzed for depth and roughness using an optical profilometer (Zygo, Middlefield, CT, USA). It should be noted that it is possible for the etching procedure to produce very small quantities of HF and thus appropriate handling procedures should be used. Optical profilometry gives high resolution three-dimensional images of surfaces by measuring the interference fringes generated from the reflection of polarized white light from the surface.[19]

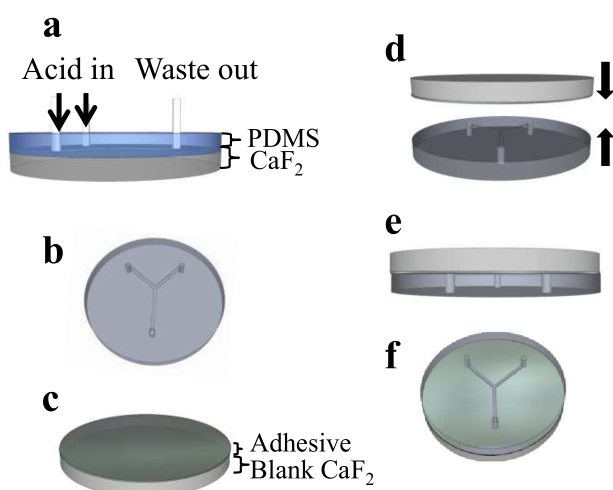

Figure 1. CaF_2 microfluidic device fabrication process. **(a)** PDMS mold is used to direct the flow of 1.5 M nitric acid over 25-mm diameter CaF_2 plate. **(b)** 1-mm inlet and outlet holes are drilled into the completed etch. **(c)** 700-nm thick adhesive layer of PDMS and toluene (1:6) is spin coated onto a non-etched CaF_2 plate. **(d)** The etched plate and plate with adhesive layer are clamped together and oven cured for 1 hr. **(e)** Side view of device. **(f)** Completed microfluidic device.

Sealing of microfluidic devices. Once the etch was completed, inlet and outlet holes were drilled with 1 mm diamond-tipped drill bits (Diamond Pacific Tool Corp., Barstow, CA, USA) in a high-speed drill press. PDMS was diluted in a 1:6 ratio with toluene and spin-coated (90 s at 1500 rpm with 700 rpm/s acceleration) onto an unetched CaF_2 plate. The PDMS-coated plate

Lab on a Chip Accepted Manuscript

was then brought into conformal contact with an etched, uncoated CaF_2 plate (Figure 1d-f). The plates were clamped together with a 3D-printed holder, and thermally cured at 80 °C for 1 hr. After curing, the holder was removed, inlet/outlet tubing was inserted into the inlet and outlet holes and sealed with partially cured, undiluted PDMS. After PDMS curing, the device was ready for use without any need for an external clamping device. Profilometer data taken of the spin-coated PDMS layer before it was pressed onto the etched CaF_2 shows that the PDMS layer was 670 ± 280 nm thick (Figure S1), which is in agreement with the results of Wu *et al.*[20] The PDMS adhesive is strong enough to hold the two CaF_2 plates together without an external clamping device while having minimum absorbance in the IR region (Figure S2).

FTIR Spectroscopic Imaging. FTIR data was obtained using a Bruker Hyperion 3000 FTIR microscope (Bruker Optics, Billerica, MA, USA) equipped with a 15X objective and a 64 x 64 focal plane array (2.6 μm/pixel), which enables 4,096 spectra to be taken over a 165 μm x 165 μm area. The microscope was outfitted with a computer controlled *xy* stage to allow for image stitching. Spectral resolution was set at 4 cm^{-1} and 32 scans were taken for each sample area in transmission mode. The microfluidic device used in these FTIR experiments had an average depth of 29 ± 1.3 μm (n=1150 points along channel), average main channel width of 563 ± 85 μm (n=4 points from single cross-sectional area), and channel length of 8.3 mm. Solutions of 0.5 M NMA in dimethyl sulfoxide and D_2O were mixed at a flow rate of 1 μL/min in each channel using the CaF_2 microfluidic described above.

Results and Discussion

Lab on a Chip Accepted Manuscript

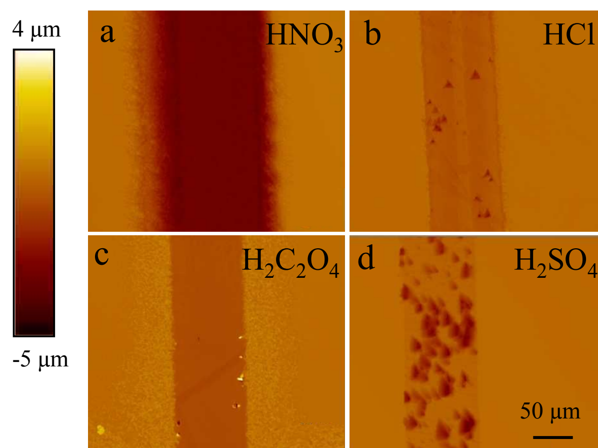

Figure 2. Optical profiles of 100-µm wide channels etched into CaF_2 at 1 µL/min. **(a)** 0.1 M nitric acid at 12 hr. **(b)** 0.1 M hydrochloric acid at 15 hr. **(c)** 0.28 M oxalic acid at 18 hr. **(d)** 0.1 M sulfuric acid at 12 hrs.

Etching conditions. The impact of sulfuric, hydrochloric, oxalic, and nitric acids on CaF_2 etching was studied to determine the best acid etchant for CaF_2. These acids were chosen based on previous reports except for oxalic acid, which can act as a bidentate ligand, a conjugate base, and can bind with calcium.[21] Figure 2 shows optical profilometry images of etches done with each acid. Nitric acid provided a relatively smooth, deep channel with the lowest surface roughness (S_a), while hydrochloric and sulfuric acid gave rough, pitted channels (Table 1). Oxalic acid also gave a smooth channel but the overall etch rate was slower than nitric acid and thus it was not used for further experiments. However, if very smooth, shallow channels are desired, this is a viable etchant as well. Etching rates were calculated for all acids based on the average channel depth (29 µm) with a total channel surface area of roughly 5000 μm^2. Measurements were taken in the flat sections of the channel away from the channel edges. Pits found in the sulfuric and hydrochloric etches deeper than 0.8 µm were not taken into account during the calculation because of steep surfaces that prevented accurate depth measurements in some pits. Since nitric acid gave the highest etch rate and smallest S_a, it was used in all further etching.

Lab on a Chip Accepted Manuscript

Table 1. Acidic solutions used to etch CaF_2 plates at 1 µL/min using a PDMS template. N=1 for each acid etch. >0.8 µm pits found in the hydrochloric and sulfuric acid etches were not taken into account during image analysis.

Acid	Average Etch Rate (µm/hr)	S_a* (µm)	Concentration (M)	pH
HNO_3	0.27	0.58	0.10	1.1
HCl	0.04	2.44	0.10	1.1
$H_2C_2O_4$	0.04	0.74	0.28	1.0
H_2SO_4	0.01	0.70	0.10	1.2

*Mean surface roughness measurement

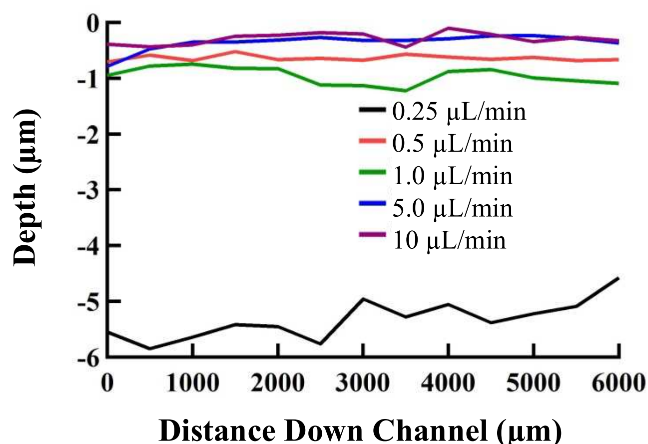

Figure 3. Average depth of etched CaF_2 with 100-µm wide channel etched CaF_2 with 0.1 M nitric acid plotted against the length of the channel.

Etch rate. The depth of the etched channel is controlled by the acid concentration, flow rate, and total volume. We tested the effect of flow rates by varying rates from 0.25 to 5 µL/min while keeping the volume of fluid constant 1 mL. Figure 3 shows that slow flow results in a deeper etch depth, which is expected given the longer total acid exposure time. Furthermore, for the slowest flow rate, the channel was noticeably shallower at the end of the channel than the beginning. We are unsure of the exact mechanism but suspect this could be due to changes in

Lab on a Chip Accepted Manuscript

linear velocity as the entrance of the channel is etched first and therefore the flow is slower in that region given the use of constant flow volume syringe pumps for this process. Figure 4 shows the correlation between etching time and the resulting channel depth; as expected the longer etching times resulted in deeper channels. 8, 12, 16 and 20 hr etches were plotted showing the depth of 3 different trials, but 4, 24, and 48 hr etches with only a single etch are plotted as well. Linear regression, prediction and confidence bands were plotted for all data points. There is variability between etches of the same time length which results in cumulative standard deviation of 1.4 μm for all etch times averaged together. Further testing needs to be done to understand the factors leading to the variability. Finally, the optimized conditions were used to etch a Y-channel into CaF_2 and the resulting structure was analyzed by optical profilometry (Figure 5). The process created a well-defined channel with a depth of 8 μm. Additional examples of other channel geometries are shown in Figures S5-S8 in the supplementary material, including 90° angles, curved turns, channels with a range of widths, oval bubble cells, and an angled bubble cell similar to what has been used previously for improved conductometric detection in electrophoresis.[22]

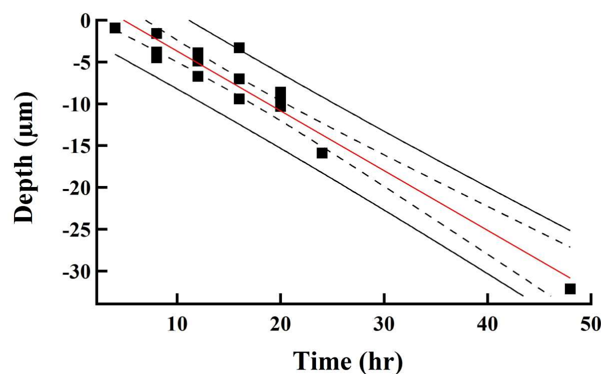

Figure 4. Etch depth as a function of time when utilizing 1.5 M nitric acid.

Lab on a Chip Accepted Manuscript

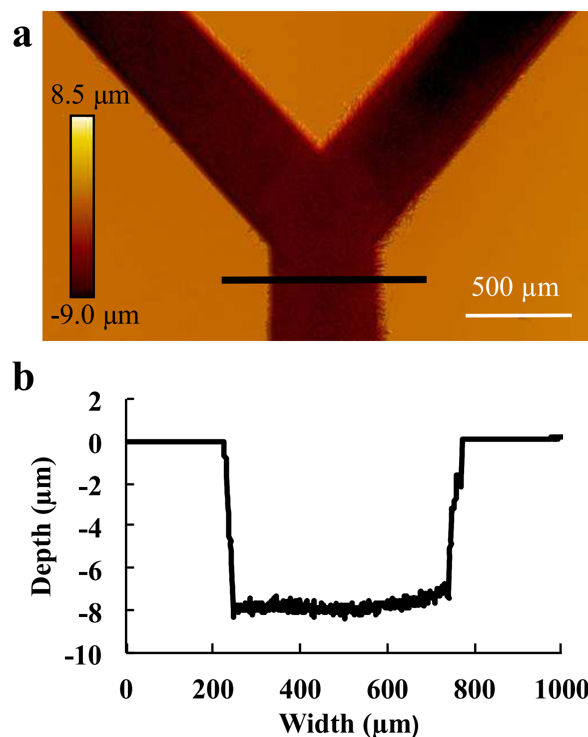

Figure 5. (a) Optical profile of 12-hr etch at 0.25 µL/min using PDMS mold with 500-µm wide channels and 1.5 M nitric acid. **(b)** Line-scan profile of area indicated with the black line in Figure 2a.

IR-transparent microfluidics with channel heights ranging from 6 µm to 75 µm tall have been reported previously.[23, 10] Microfluidics used to study proteins typically have a channel heights below 10 µm to decrease the water absorbance peak which can overlap with amide bond vibrations.[23] D_2O is sometimes used in place of H_2O because it has a lower interference with the amide bond peak, allowing for channel heights of 50 µm to be used when studying proteins.[24] One benefit of the new method is that the height of the channel can be easily controlled by etching time, flow rate, and/or acid strength enabling use of these devices in many applications.

Infrared spectroscopy. To demonstrate utility, a CaF_2 chip (Figure 6a) was used with an FT-IR microscope to follow an amide bond response to deuterated water. NMA in DMSO and D_2O

Lab on a Chip Accepted Manuscript

were added separately through legs of a Y-channel and mixed at a combined flow rate of 2 μL/min in the third arm of the system where spatially resolved FTIR spectra were collected. This is a similar H-D exchange experiment is done by Kazarian and coworkers with H_2O-D_2O to form HOD,[25] except the H-D exchange being monitored was on NMA amide. Figure 6 shows a photograph of the device (6a) with the locations of the data acquisition as well as intensity-position-wavenumber maps (6b and c). In Figures 6b and 6c, the position refers to the vertical position in the channel with position 0 corresponding to the top of the channel. The color intensity corresponds to the absorbance at a given wavenumber, and a single spectrum could be obtained by extracting the data along any horizontal line in the figure. This format was selected for plotting the results because it allows easy visualization of peak absorbance shifts relative to position. The amide peak shift from 1650 cm^{-1} to 1625 cm^{-1} can be observed as the solutions diffusively mix together along the channel. The downward peak shift resulting from the introduction of NMA into a deuterated environment is clearly seen, and the band is fully shifted to 1625 cm^{-1} roughly 4 mm down the channel. FTIR spectra of the actual peak shift with a corresponding image of the channel along with spectra from different positions along the channel can be seen in Figures S3 and S4. These results clearly demonstrate the ability of this system to follow a chemical reaction using the etched CaF_2 devices.

Lab on a Chip Accepted Manuscript

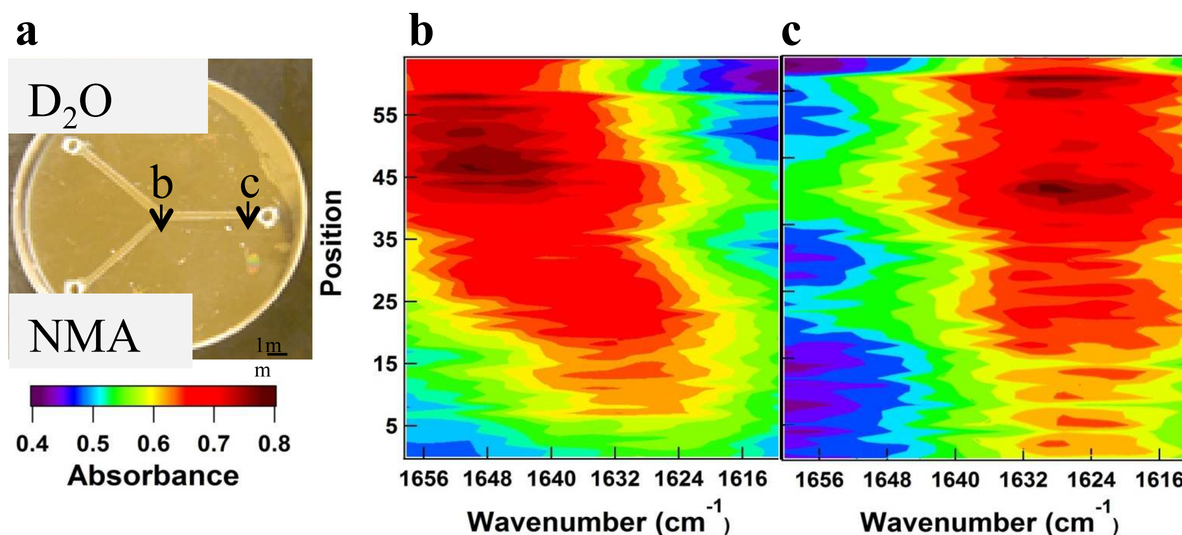

Figure 6. **(a)** Image of the CaF_2 microfluidic device used in experiments. Arrows indicate the direction in which data was obtained. **(b)** Wavenumber intensity plot of FTIR data taken at "b", 200 µm down from start of channel, indicated in Figure 6a. **(c)** Wavenumber intensity plot of FTIR data taken at "c", 4000 µm down from start of channel, indicated in Figure 6a.

Conclusions. Previous reports of IR-transparent CaF_2 microfluidic devices have relied primarily on additive fabrication methods. The single method based on etching of CaF_2 reported by the Woolley group used traditional photolithography and $Fe(NH)_4(SO_4)_2$ as the etchant to define channels. While this approach was successful at generating devices that could be used for capillary electrophoresis and IR spectroscopy, the use of traditional lithography to fabricate each channel requires expensive photolithography equipment. Here, channels fabricated by soft lithography in PDMS were reversibly sealed over an unpatterned CaF_2 substrate and nitric acid pumped through the microfluidics. The acid anisotropically etches a Y-channel into the CaF_2 allowing for simple fabrication of etched CaF2 microfluidic devices. The method allows for simple fabrication of devices using traditional PDMS microfluidic devices and has the ability to make intricate fluidic networks when compared to other similarly formed CaF_2 chips.

Lab on a Chip Accepted Manuscript

Acknowledgements: The authors would like to thank Michael Barich for his help with Matlab programming. This work was funded by a contract from BP.

Lab on a Chip Accepted Manuscript

References

1. G. S. Jeong, S. Chung, C. B. Kim and S. H. Lee, *Analyst*, 2010, **135**, 460-473.
2. V. Hessel, H. Lowe and F. Schonfeld, *Chemical Engineering Science*, 2005, **60**, 2479–2501.
3. G. A. M. David J. Beebe, and and G. M. Walker, *Annual Review of Biomedical Engineering*, 2003, DOI: 10.1146/annurev.bioeng.4.112601.125916.
4. P. Hinsmann, M. Haberkorn, J. Frank, P. Svasek, M. Harasek and B. Lendl, *Applied Spectroscopy*, 2001, **55**, 241-251.
5. N. Kaun, M. J. Vellekoop and B. Lendl, *Applied Spectroscopy*, 2006, **60**, 1273-1278.
6. M. Kakuta, P. Hinsmann, A. Manz and B. Lendl, *Lab Chip*, 2003, **3**, 82-85.
7. P. Hinsmann, J. Frank, P. Svasek, M. Harasek and B. Lendl, *Lab Chip*, 2001, **1**, 16-21.
8. K. L. A. Chan and S. G. Kazarian, *Anal. Chem.*, 2012, **84**, 4052-4056.
9. K. L. A. Chan, X. Z. Niu, A. J. de Mello and S. G. Kazarian, *Lab Chip*, 2010, **10**, 2170-2174.
10. D. P. Kise, D. Magana, M. J. Reddish and R. B. Dyer, *Lab on a Chip*, 2014, **14**, 584-591.
11. C. Wagner, W. Buchegger, M. Vellekoop, M. Kraft and B. Lendl, *Anal. Bioanal. Chem.*, 2011, **400**, 2487-2497.
12. M. V. Barich and A. T. Krummel, *Anal. Chem.*, 2013, **85**, 10000-10003.
13. E. Mitri, A. Pozzato, G. Coceano, D. Cojoc, L. Vaccari, M. Tormen and G. Grenci, *Microelectronic Engineering*, 2013, **107**, 6-9.
14. T. M. Floyd, M. A. Schmidt and K. F. Jensen, *Industrial & Engineering Chemistry Research*, 2005, **44**, 2351-2358.
15. E. Mitri, G. Birarda, L. Vaccari, S. Kenig, M. Tormen and G. Grenci, *Lab on a Chip*, 2014, **14**, 210-218.
16. T. Pan, R. T. Kelly, M. C. Asplund and A. T. Woolley, *J. Chromatogr. A*, 2004, **1027**, 231-235.
17. Y. X. G. M. Whitesides, *Annual Review of Materials Science*, 1998, **28**, 153-184.
18. D. C. Duffy, J. C. McDonald, O. J. Schueller and G. M. Whitesides, *Anal Chem*, 1998, **70**, 4974-4984.
19. P. d. Groot, *Advances in Optics and Photonics, Vol. 7, Issue 1, pp. 1-65*, 2015, **7**, 1-65.
20. H. Wu, B. Huang and R. N. Zare, *Lab on a Chip*, 2005, DOI: 10.1039/B510494G, 1393-1398.
21. C. Motzer and M. Reichling, *Journal*, 2009, **105**, 064309.
22. S. D. Noblitt and C. S. Henry, *Anal. Chem.*, 2008, **80**, 7624-7630.
23. F. Dousseau, M. Therrien and M. Pezolet, *Applied Spectroscopy*, 1989, **43**, 538-542.
24. J. Kong and S. Yu, *Acta Biochim Biophys Sin (Shanghai)*, 2007, **39**, 549-559.
25. K. L. A. Chan, S. Gulati, J. B. Edel, A. J. de Mello and S. G. Kazarian, *Lab Chip*, 2009, **9**, 2909-2913.

Lab on a Chip Accepted Manuscript